Rational construction of genome-minimized *Streptomyces* host for the expression of secondary metabolite gene clusters

Hui Li [a,1], Sheng Gao [a,1], Sanyuan Shi [b,1], Xiaomin Zhao [b], Haoyu Ye [a], Yunzi Luo [a,b,c,d,*]

[a] *Department of Gastroenterology, State Key Laboratory of Biotherapy, West China Hospital, Sichuan University, Chengdu, 610041, China*
[b] *Frontiers Science Center for Synthetic Biology and Key Laboratory of Systems Bioengineering (Ministry of Education), School of Chemical Engineering and Technology, Tianjin University, Tianjin, 300072, China*
[c] *Georgia Tech Shenzhen Institute, Tianjin University, Tangxing Road 133, Nanshan District, Shenzhen, 518071, China*
[d] *Haihe Laboratory of Sustainable Chemical Transformations, Tianjin, 300192, China*

A B S T R A C T

Streptomyces offer a wealth of naturally occurring compounds with diverse structures, many of which possess significant pharmaceutical values. However, new product exploration and increased yield of specific compounds in *Streptomyces* have been technically challenging due to their slow growth rate, complex culture conditions and intricate genetic backgrounds. In this study, we screened dozens of *Streptomyces* strains inhabiting in a plant rhizosphere for fast-growing candidates, and further employed CRISPR/Cas-based engineering techniques for stepwise refinement of a particular strain, *Streptomyces* sp. A-14 that harbors a 7.47 Mb genome. After strategic removal of nonessential genomic regions and most gene clusters, we reduced its genome size to 6.13 Mb, while preserving its growth rate to the greatest extent. We further demonstrated that cleaner metabolic background of this engineered strain was well suited for the expression and characterization of heterologous gene clusters, including the biosynthetic pathways of actinorhodin and polycyclic tetramate macrolactams. Moreover, this streamlined genome is anticipated to facilitate directing the metabolic flux towards the production of desired compounds and increasing their yields.

1. Introduction

The genus *Streptomyces*, which is part of the family *Streptomycetaceae*, was an industrially prominent microorganism that produces a large portion of antibiotics, and other biologically active secondary metabolites [1–3]. However, the original *Streptomyces* producers of desired products often grow poorly, lack intractable genetic engineering tools, and have complicated metabolic backgrounds [4,5]. Synthetic biology strategies can improve yield or activate the production of bioactive compounds by cloning the biosynthetic gene clusters (BGCs) for heterologous expression in a well-designed and engineered microbial cell factories [6,7]. Recent advances in large BGC cloning techniques resulted successful construction of 47 BGCs and the lead to the discovery of previously uncharacterized NPs [8]. However, robust chassis for heterologous expression of these BGCs are still in limited amount.

For heterologous overproduction of valuable natural products (NPs),

Streptomyces species are selected as suitable chassis due to their sufficient supply of precursors, and adaptive regulatory mechanisms [9–11]. Therefore, genome-reduced derivatives of *Streptomyces* spp., have been constructed and widely used for heterologous expression of actinobacterial BGCs [12]. *Streptomyces coelicolor* ZM12 and *Streptomyces lividans* TK24 were constructed by deleting the endogenous BGCs to increase secondary metabolite productions [13,14]. *Streptomyces avermitilis* was an industrial producer of the anthelmintic agent avermectin. The left sub-telomeric chromosome region and several BGCs of *S. avermitilis* were deleted, generating *S. avermitilis* SUKA17, which was used for the production of several secondary metabolites with 3 to 5-fold improved yields [15]. *S. albus* J1074 has a small genome size of 6.8 Mb [16]. By removing 15 gene clusters in its genome, a mutant *S. albus* Del14 was generated, facilitating the discovery and production of NPs [17]. However, most of the engineered *Streptomyces* chassis grow slower, hindering the efficient production of NPs. Thus, an ideal *Streptomyces*

---

chassis with fluent genetic manipulation, clean metabolic background, and higher success rate of BGC expressions is in urgent need [18].

Recent advances in genome sequencing have revealed that more than 20 BGCs are distributed on each *Streptomyces* chromosome, which are usually "silent" under conventional experimental conditions [19]. Besides, pan-genome analysis revealed that each *Streptomyces* genome contains an essential genome and a dispensable genome, and deletion of the dispensable genome would not affect either growth or the primary metabolism [20]. Thus, deletion of BGCs and the nonessential genomic regions would generate a relatively clean metabolic background to improve NPs production and discovery [21]. In this study, we screened a fast-growing *Streptomyces* sp. A-14 and sequenced its genome. We strategically removed the nonessential genomic regions and some BGCs to rationally reduce its genome size to 6.13 Mb, generating a series of genome reduced strains with cleaner metabolic background and higher transformation efficiency. We successfully expressed the biosynthetic pathways of actinorhodin and polycyclic tetramate macrolactams (PTM) in the engineered chassis, with improved yields. In summary, this genome-reduced *Streptomyces* sp. A-14 strains, devoid of most endogenous natural products, holds promise for directing the metabolic flux towards the production of desired compounds with increased yield, as well as the detection of metabolic compounds produced by uncharacterized gene clusters of other *Streptomyces* origins, expanding the existing set of *Streptomyces* surrogate hosts.

2. Materials and methods

2.1. Strains, plasmids and culture conditions

The strains and plasmids used were listed in Table S1. *Escherichia coli* strains were cultured in Luria Bertani (LB) medium (10 g/L tryptone, 5 g/L yeast extract, and 10 g/L NaCl) at 37 °C. *E. coli* DH5 alpha was utilized for cloning experiments. *E. coli* ET12567 (pUZ8002) was used for conjugal transfer of plasmids from *E. coli* to *Streptomyces*. *Streptomyces* strains were cultured in MYG liquid medium (10 g/L malt extract broth, 4 g/L yeast extract, and 4 g/L glucose). MISP4 agar medium (1 g/L yeast extract, 2 g/L tryptone, 5 g/L soluble starch, 5 g/L D-mannitol, 5 g/L soya flour, 1 g/L NaCl, 2 g/L $(NH_4)_2SO_4$, 1 g/L K_2HPO_3, 2 g/L $CaCO_3$, 20 g/L agar, 1 g/L $FeSO_4$, 1 g/L $MnCl_2$, 1 g/L $ZnSO_4$ and 25 mM $MgCl_2$, pH 7.0) was used for *Streptomyces* sporulation at 30 °C. R2YE liquid medium (103 g/L Sucrose, 10 g/L glucose, 5 g/L yeast extract, 100 mg/L casamino acids, 3 g/L proline, 10 g/L $MgCl_2$·$6H_2O$, 4 g/L of $CaCl_2$·$2H_2O$, 200 mg/L of K_2SO_4, 50 mg/L of KH_2PO_4, 5.73 g/L of TES, and 2 mL trace elements) (lacking $CaCl_2$, KH_2PO_4, and L-proline) was used for the detection of actinorhodin production. For growth curve measurement, *Streptomyces* spp. strains were cultivated in SMM, NMMP, MM, YEME, and MYG liquid medium [22].

2.2. Complete genome sequencing and bioinformatics analysis

The sequencing of *Streptomyces* sp. A-14 genome was performed by Beijing Genomics Institute (BGI, Shenzhen, China). The genomic DNA was fragmented to an average size of 8–10 kb and sequenced using PacBio RS II and Illumina platforms [23]. In addition, the PacBio consensus calling feature was adopted for the correction of PacBio long reads, which could resolve highly similar repetitive sequences [24]. The final genome sequence was assembled by using hierarchical genome-assembly process (HGAP) software [25]. The protein-coding sequences (CDSs) were determined by the prediction of glimmer 3, and their functions were annotated by searching the National Center for Biotechnology Information (NCBI) and the Kyoto Encyclopedia of Genes and Genomes (KEGG) protein databases [26]. The Clusters of Orthologous Groups of proteins (COG) database, Non-Redundant protein databases (NR) and KEGG were used to analyze the function of the annotated genes [27]. Additionally, genes involved in secondary metabolite production in *Streptomyces* sp. A-14 were predicted by using antiSMASH 7.0

online software (Table S2) [19]. The complete genome sequence of *Streptomyces* sp. A-14 has been submitted to the NCBI GenBank under the BioProject ID PRJNA1083101 and the accession number CP150474.

2.3. Construction of the engineered chassis

The *Streptomyces* sp. A-14 was utilized as the parental strain, and its genome was edited using the pCRISPomyces-2 (pCM2) plasmid following its protocol [28]. The correct plasmids pCM2 (1–30) were individually transferred to *E. coli* ET12567 (pUZ8002) through heat shock and then conjugated to *Streptomyces* sp. A-14 strains, respectively. All the resulting strains were verified by PCR using primers located within or outside of the target gene clusters (Table S3). Then, sequencing of the PCR products was performed to confirm the sequences (Tsingke, Beijing, China). For clearance of the temperature-sensitive plasmid (pCM2), the correct exconjugant was cultured at 37 °C over two generations in the absence of antibiotic selection until plasmid clearance [28]. After clearance of the editing plasmids, the mutant strains of *Streptomyces* sp. A-14 (Δ1-Δ30) were obtained.

2.4. Growth analysis of Streptomyces strains

Seed culture was grown in MYG liquid medium at 30 °C with constant shaking (220 rpm) until achieving high cell density. The seed culture was then inoculated into 250 mL MYG liquid medium and cultured for five days at 30 °C. Cell density was determined by measuring the biomass dry weight. A 10 mL culture was collected in a pre-weighed centrifuge tube and immediately centrifuged at 12,000 rpm for 10 min. The residual cells were washed with distilled water and the supernatant was discarded. The pellets were dried till a constant weight at 88 °C for two days, after which the mass gain was measured. Three parallel trials of every sample were performed to determine the error bar and standard deviation.

2.5. Construction of mutant strains expressing BGCs

Gene cluster fragments were amplified from the genomic DNA of *Streptomyces* sp. A-14. The promoter *kasO**p was amplified from the plasmid pCM2. The genes with corresponding promoters were assembled by overlap extension PCR (OE-PCR). The resulting expression cassettes were cloned into shuttle vectors pYES using DNA assembler [29]. The purified plasmids from *E. coli* were subjected to restriction digestion. The plasmids with reconstructed gene clusters were transferred to *Streptomyces* chassis cells via conjugation.

2.6. Measurement of the actinorhodin production

To quantify the production of actinorhodin, $1*10^9$ spores were incubated in R2YE liquid medium supplemented with 20 μg/mL apramycin and 40 μg/mL nalidixic about 10 days at 30 °C. Afterwards, 0.75 mL culture was harvested, and treated with 250 μL of 3 M KOH. The mixture was vortexed thoroughly and then centrifuged at $4000 \times g$ for 10 min. The absorption of the supernatant was measured at $\lambda = 640$ nm [30].

2.7. Fermentation, extraction and analysis of PTMs

Aliquots of the seed culture with a volume of 250 μL were spread for confluence over MYG solid medium plates, and the plates were inoculated at 30 °C for 7 days. To isolate potential compounds, the plates were stored at −25 °C for one day, after which the thawed cultures were squeezed completely and the released liquids were extracted using ethyl acetate. Extracts were dried under reduced pressure, resuspended in 1 mL methanol, and analyzed using HPLC (Agilent Technologies Inc., Carpinteria, CA, United States) and LC-MS (Agilent Technologies Inc., AB SCIEX X500R QTOF, United States). HPLC parameters were as

follows: solvent A, 0.1 % formic acid in the water, solvent B, acetonitrile; gradient, 10 % B for 5 min, to 100 % B in 25 min, maintain at 100 % B for 10 min, return to 10 % B in 1 min and finally maintain at 10 % B for 9 min; flow rate 0.5 mL/min; detection by UV wavelength at 320 nm.

3. Results

3.1. The screening of Streptomyces sp. A-14

We isolated *Streptomyces* sp. A-1 to A-18 from the rhizosphere of the herb *Ferula sinkiangensis* in Xinjiang province (84°57′-86°09′E, 43°29′-45°20′N). *Streptomyces* strains generally have a long growth cycle and complex metabolic backgrounds [31]. We cultured strain *Streptomyces* sp. A-1 to A-18 on MISP4 agar plates and measured its growth curves in MYG liquid medium. *Strepto*myces sp. A-5, *Strepto*myces sp. A-8 *Streptomyces* sp. A-14 and *Strepto*myces sp. A-18 exhibited obvious aerial and substrate mycelia on the first day. Among them, *Strepto*myces sp. A-14 showed the fastest sporulation rate and no signs of pigment formation on the third day. Meanwhile, *Streptomyces* sp. A-14 can form single colonies on MISP4 solid agar plates, and has a faster sporulation rate compared to *S. albus*, *S. coelicolor*, *S. lividans*, and *S. avermitilis* (Fig. S1). We selected the fast-growing *Streptomyces* sp. A-5, A-8, A-14, A-18 and *S. venezuelae* to test their growth curves, and found that *Streptomyces* sp. A-14 grew faster than *Streptomyces* sp. A-5, A-8, A-18 and *S. venezuelae* (Fig. 1). In this study, *Streptomyces* sp. A-14 was selected as a candidate for chassis construction.

3.2. Genomic analysis of Streptomyces sp. A-14

Further phylogenetic analysis based on 16S rRNA gene sequences revealed that *Streptomyces* sp. A-14 was closely related to *Streptomyces badius* NRRL B-2567 (99.93 %). The complete genome sequence of *Streptomyces* sp. A-14 was obtained using the PacBio SMRT and Illumina sequencing platforms. The linear chromosome comprises 6762 predicted genes, and the length of genes majorly ranged from 100 to 2000 bp (Fig. S2A), including 6 ribosomal RNA (rRNA) genes, 67 transfer RNA (tRNA) genes, and 8 small RNA (sRNA) genes, and could be visualized in the circular map by Circos (Fig. 2A). Genome assembly sequences revealed that the size of *Streptomyces* sp. A-14 genome was 7.47 Mb, with an average GC content of 71.65 % (Fig. S2B). The replication origin (*oriC*) and *dnaA box-like* (encoded by A-14AGL003469) were located at 3,717,170–3,719,023 bp with a 0.84 Mb deviation to the center, indicating asymmetry of the chromosome structure. In addition, the *Streptomyces* sp. A-14 genome harbors a linear plasmid with a total length of 205,884 bp, and the GC content was 68.97 % (Fig. 2B).

Genome analysis via antiSMASH 7.0 revealed 33 putative secondary metabolite BGCs (1,015,382 bp in total), accounting for 13.59 % of the genome. The majority of these gene clusters were distributed in sub-telomeric regions (Table S2). Based on the analysis of the location of the BGCs, 17 BGCs dispersed in the 0–2.2 Mb and 4.4–7.26 Mb regions were selected as deletion candidate regions.

Pan-genome analysis was further performed to determine the core genes, dispensable genes, and strain-specific genes in given genomes [32]. 80 divergent *Streptomyces* species were selected for pan-genome analysis (Table S4), and the core genome is most scattered in the middle of the chromosome (Fig. S2C). About 846 genes are well conserved in all 80 genomes, particularly appeared at 1.63–4.4 Mb, which may belong to putative essential genes, and the number of core genes gradually decreased along with the increasing number of given genomes (Fig. S2D). The vast majority of dispensable genes dispersed in sub-telomeric regions, which were not necessary for primary metabolism and robust cellular functions. Consequently, several candidate genomic regions scattered on the arms of the chromosome (0–1.63 Mb and 4.4–7.26 Mb) were selected to be removable.

3.3. Construction of genome-reduced Streptomyces sp. A-14 chassis strains

According to the genomic analysis, 37 regions were selected to be deleted from the *Streptomyces* sp. A-14 chromosome (Table 1). The previously established CRISPR-Cas9 genome editing system was applied to enable defined editing via homologous recombination (Fig. 3A) [28]. Two 2 kb homologous arms cloned from the corresponding upstream and downstream sequences of the protospacer, were assembled into pCM2. 30 regions, including gene clusters 1, 2, 3, 4, 5, 6, 7, 8, 10, 11, 13, 16, 23, 25, 26, 28, 29, 30 (Table S2) and several non-essential genomic regions, were successfully deleted and labeled as genome-reduced strains *Streptomyces* sp. A-14 Δ1-Δ30 (Fig. 3B, Table 1). The successfully deletion mutants were confirmed by PCR and sequencing (Fig. 3C). The deletion sizes range from 7 to 73.3 kb, with efficiencies of 12.5–90.9 %, respectively.

The successfully deleted regions were mainly distributed in the left sub-telomeric of the genome. The regions scattered in the middle regions of the chromosome were difficult to be deleted. Among the 31 predicted BGCs in *Streptomyces* sp. A-14 chromosomes, 25 dispensable BGCs were chosen but only 18 were successfully deleted. Ultimately, Δ30 genome was reduced by 1338 kb (17.9 % of the entire genome) compared with that of the parental *Streptomyces* sp. A-14 strain, resulting in the lost ability to synthesize most indigenous secondary metabolites.

3.4. Characterization of the genome-reduced Streptomyces sp. A-14 strains

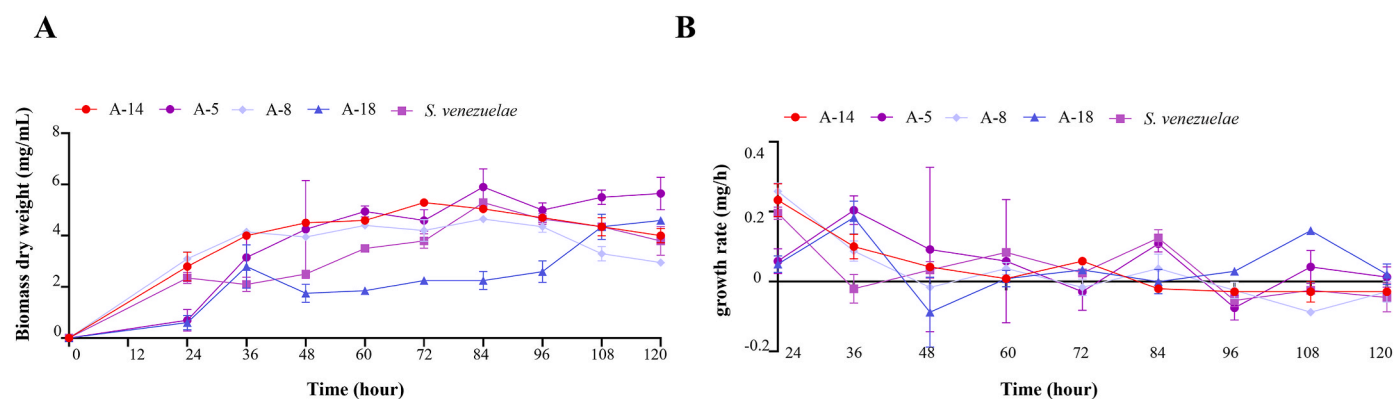The growth of all *Streptomyces* sp. A-14 mutant stains in the complex

Fig. 1. The growth characterization of *Streptomyces* strains screen from plant rhizosphere of the herb *Ferula sinkiangensis*. (A) The growth curves of the *Streptomyces* sp. A-5, *Streptomyces* sp. A-8, *Streptomyces* sp. A-14, *Streptomyces* sp. A-18, and *S. venezuelae* were measured by biomass in MYG liquid culture. (B) The growth rates of the isolated *Streptomyces* sp. A-5, *Streptomyces* sp. A-8, *Streptomyces* sp. A-14, *Streptomyces* sp. A-18 and *S. venezuelae* were measured by biomass in MYG liquid culture.
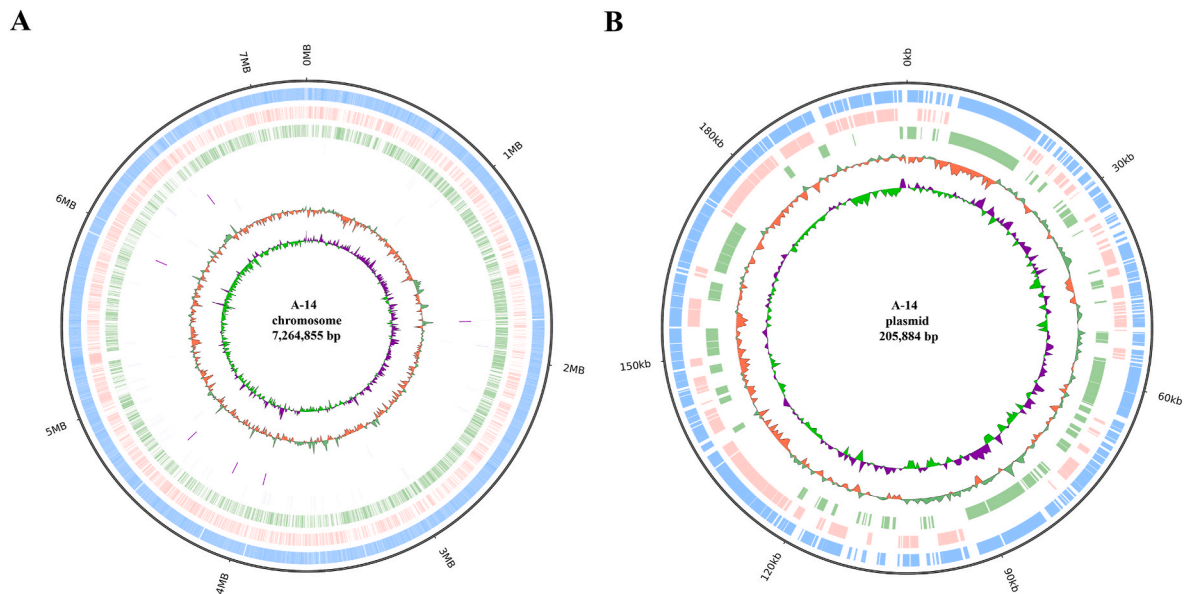
Fig. 2. Circular genome map of the *Streptomyces* sp. A-14 genome and plasmid. (A) The chromosome atlas. From inner to outer, 1, Genome Size; 2. all anno gene; 3 and 4, displayed the CDSs on the forward strand (red) and reverse strand (green); 5, 6, and 7, displayed tRNA, rRNA, sRNA; 8, GC content; 9, GC skew. (B) Atlases of linear plasmid. 1, Genome Size; 21, all anno gene; 3 and 4, displayed predicted genes (reverse and forward strands, respectively); 5, GC percentage plot (±); 6, GC skew. The genome and plasmid map made by using Circos.

Table 1
The regions deleted in the chromosome of the *Streptomyces* sp. A-14 strain.

Strain ID	Positions	Size of deleted regions (bp)	Deletion gene cluster	Coordinates of deleted genes	Chromosome sizes (bp)	Ratio (%)
Wild type	–	–			7470739	
Δ1	141,980–207,203	65224	Cluster 3	AGL000130-AGL000180	7405515	99.13
Δ2	387,933–428,582	40650	Cluster 5	AGL000361-AGL000398	7364865	98.58
Δ3	2067–64,746	62680	Cluster 1	AGL000004-AGL000060	7302185	97.74
Δ4	270,163–343,491	73329	Cluster 4	AGL000246-AGL000312	7228856	96.76
Δ5	4,847,751–4,916,614	68864	Cluster 25	AGL004491-AGL004553	7159992	95.84
Δ6	1,057,480–1,086,061	28582	Cluster 11	AGL000985-AGL001009	7131410	95.46
Δ7	1,163,320–1,230,479	67160	a	AGL001082-AGL001139	7064250	94.56
Δ8	209,198–268,145	58948	Cluster 3	AGL000183-AGL000243	7005302	93.77
Δ9	7,106,586–7,126,719	20134	Cluster 30	AGL006605-AGL006622	6985168	93.50
Δ10	7,005,815–7,064,833	59019	Cluster 29	AGL006516-AGL006571	6926149	92.71
Δ11	5,847,413–5,854,556	7144	Cluster 26	AGL005359-AGL005365	6919005	92.61
Δ12	66,793–110,376	43584	Cluster 2	AGL000063-AGL000094	6875421	92.03
Δ13	112,328–140,031	27704	a	AGL000097-AGL000129	6847717	91.66
Δ14	983,729–1,001,547	17819	Cluster 10	AGL000917-AGL000934	6829898	91.42
Δ15	601,602–655,627	54026	Cluster 7	AGL000562-AGL000616	6775872	90.70
Δ16	6,965,712–7,001,737	36026	Cluster 28	AGL006479-AGL006512	6739846	90.22
Δ17	430,592–496,296	65705	a	AGL000401-AGL000461	6674141	89.34
Δ18	519,217–569,077	49861	a	AGL000487-AGL000525	6624280	88.67
Δ19	891,070–961,328	70259	a	AGL000839-AGL000898	6554021	87.73
Δ20	1,381,633–1,429,361	47729	a	AGL001283-AGL001313	6506292	87.09
Δ21	676,607–691,674	15068	Cluster 8	AGL000640-AGL000644	6491224	86.89
Δ22	6,928,640–6,963,579	34940	Cluster.28	AGL006449-AGL006476	6456284	86.42
Δ23	1,431,320–1,488,278	56959	Cluster 13	AGL001315-AGL001380	6399325	85.66
Δ24	570,924–599,510	28587	a	AGL000529-AGL000559	6370738	85.28
Δ25	1,276,193–1,320,413	44221	a	AGL001189-AGL001224	6326517	84.68
Δ26	345,545–385,986	40442	Cluster 4	AGL000319-AGL000359	6286075	84.14
Δ27	1,602,629–1,635,876	33248	a	AGL001283-AGL001311	6252827	83.70
Δ28	1,232,689–1,267,326	34638	a	AGL001143-AGL001178	6218189	83.23
Δ29	2,076,764–2,114,925	38162	Cluster 16	AGL001882-AGL001913	6180027	82.72
Δ30	4,432,806–4,480,179	47374	Cluster 23	AGL004120-AGL004161	6132653	82.09

Unknocked regions	Positions	Size of regions (bp)	Gene cluster	Coordinates of genes	Chromosome sizes (bp)	Ratio (%)
31	2,460,885–2,482,248	21,364	Cluster 17	AGL002229-AGL002247	NA	NA
32	2,902,011–2,925,580	23,570	Cluster 19	AGL002653-AGL002671	NA	NA
33	4,793,836–4,845,900	52,065	Cluster 24	AGL004439-AGL004488	NA	NA
34	3,831,087–3,874,232	43,146	a	AGL003571-AGL003598	NA	NA
35	3,114,678–3,135,573	20,896	Cluster 21	AGL002860-AGL002878	NA	NA
36	1,546,271–1,600,764	54,494	a	AGL001424-AGL001474	NA	NA
37	1,490,110–1,544,250	54,141	Cluster 14	AGL001382-AGL001422	NA	NA

a The regions in this column were not located in the gene cluster, NA: not available.
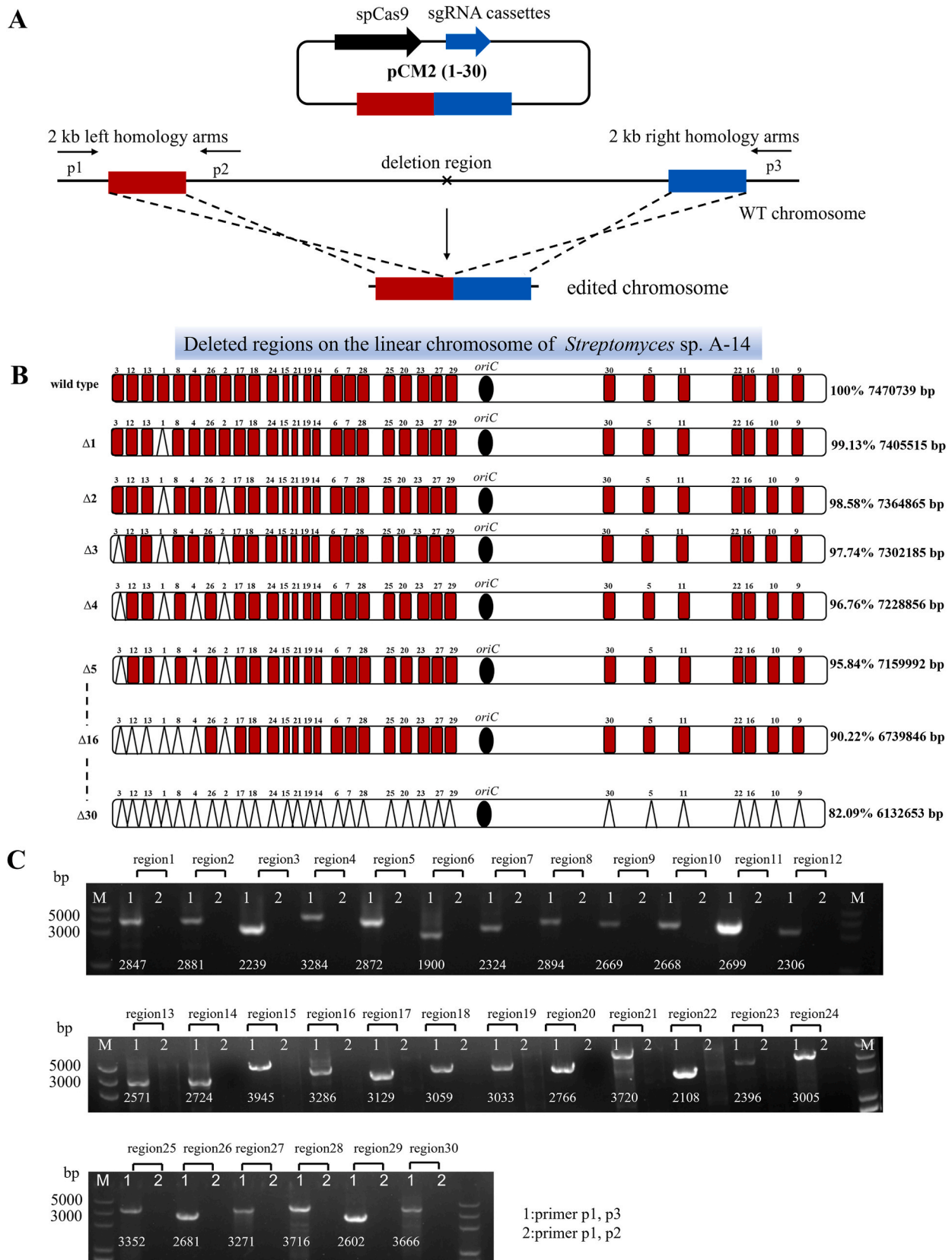
Fig. 3. The construction procedure of the genome-reduced mutants of *Streptomyces* sp. A-14 chassis. (A) Strategy for construction of large-deletion mutants and screening for the desired genotype by PCR. Cas9 introduce DSBs at middle of the gene cluster, and a co-delivered editing template bridges the gap via homologous recombination. (B) Sequential deletion of the secondary metabolic gene clusters and unknown of the linear chromosome. The *ori*C and the telomeres of the *Streptomyces* sp. A-14 linear chromosome shown, and the knock-out regions were mainly distributed in the left arm of the genome. (C) The PCR validated knock-out of 1–30 regions. Primer P1/P3 was located on the genome, and primer P2 was located on the delete region. The correct result of knock-out was that the P1/P3 had bands and the primer P1/P2 had no bands, M:5000 Marker.

media (MYG, YEME) and simple mineral media (SMM, NMMP, MM) was measured. In MYG liquid medium, the mutant strains Δ1 to Δ18 exhibited similar growth rates to that of the wild type (WT) strain, whereas strains Δ19 to Δ30 showed slower growth rate and lower biomass (Fig. 4A). In YEME and simple mineral media, the *Streptomyces* sp. A-14 strain and the genome-reduced *Streptomyces* sp. A-14 strains did not grow well, which made it difficult to measure growth curves by biomass.

We next tested the transformation efficiency of genome-reduced mutants with two plasmids, pSET152 and pCM2, respectively. For pSET152 plasmid, there were no obvious differences in transformation efficiency between *Streptomyces* sp. A-14 WT and the selected genome-reduced strains. The plasmid pCM2 contains the CRISPR/Cas9 system, which may be toxic to some *Streptomyces* strains. As a result, the efficiency of transformation of pCM2 was lower than that of the plasmid pSET152. Interestingly, the transformation efficiencies of pCM2 in the mutants (Δ6-Δ30) were approximately three times higher than that of the *Streptomyces* sp. A-14 WT strain (Fig. 4B). The deletion of regions 1–6, seems to increase the capability of accepting CRISPR/Cas9 systems to some degree.

To further examine whether the metabolic background of *Streptomyces* sp. A-14 was simplified through genome reduction, ethyl acetate and 1-butanol extracts of the *Streptomyces* sp. A-14 WT, Δ1-Δ30 strains and two commonly used deletion chassis *S. coelicolor* ZM12, *S. avermitilis* SUKA17 grown in MYG medium were analyzed via HPLC. The *Streptomyces* sp. A-14 Δ30 strain had a cleaner metabolic background compared to that of the *Streptomyces* sp. A-14 WT, *S. coelicolor* ZM12, and *S. avermitilis* SUKA17 (Fig. 4C and D). A gradual simplification of the HPLC profile was observed from the mutant strains, and Δ6-Δ30 have simpler metabolic background compare to those of the two commonly used chassis *S. coelicolor* ZM12 and *S. avermitilis* SUKA17 (Fig. S3).

3.5. Heterologous expression of the actinorhodin BGC in Streptomyces sp. A-14 chassis

Actinorhodin (ACT) is a well-characterized pH indicator metabolite (red/blue) in *S. coelicolor*, encoded by a 22 kb type II polyketide synthase (PKS) BGC, and its concentration can be measured by UV spectrophotometry [33]. To compare the productivity of the genome-reduced *Streptomyces* sp. A-14 mutants for the heterologous expression of secondary metabolic BGCs, the ACT biosynthetic gene cluster derived from *S. coelicolor* was cloned into a pYES vector by DNA assembler [29]. The resulting plasmid (pYES-ACT) was transformed into the genome-reduced strains Δ1-Δ30, as well as another two commonly used *Streptomyces* chassis *S. coelicolor* ZM12 and *S. avermitilis* SUKA17, respectively (Fig. 5A).

We measured the concentration of produced ACT in R2YE liquid medium. Compared to *Streptomyces* sp. A-14, the yields of ACT in Δ2, Δ5, Δ7, Δ16, Δ17, Δ19, Δ20 were about 1.5–3.1-fold higher, among which Δ16 had the highest ACT yield. In addition, the productions of ACT were higher in mutant strains than that of *S. avermitilis* SUKA17, especially in strains Δ2, Δ5, Δ7, Δ16, and Δ17 (Fig. 5B). The results showed that the chassis strain Δ16 was the best performing strain producing ACT, and these genome-reduced mutants (Δ2, Δ5, Δ7, Δ16, Δ17, Δ19, Δ20) significantly increased the production of PKS, which could be used as the chassis strain for PKS heterologous expression.

3.6. Activation of PTM BGC in Streptomyces sp. A-14 mutant chassis

We selected a silent gene cluster in *Streptomyces* sp. A-14 to evaluate the ability of expression NP BGCs of the mutant strains. This PTM gene cluster showed 85 % sequence identity to the PTM gene cluster in *Streptomyces griseus* (Fig. 6A). This gene cluster contained a conserved hybrid PKS-NRPS gene 2 with a size of 9.39 kb, and it is silent under the
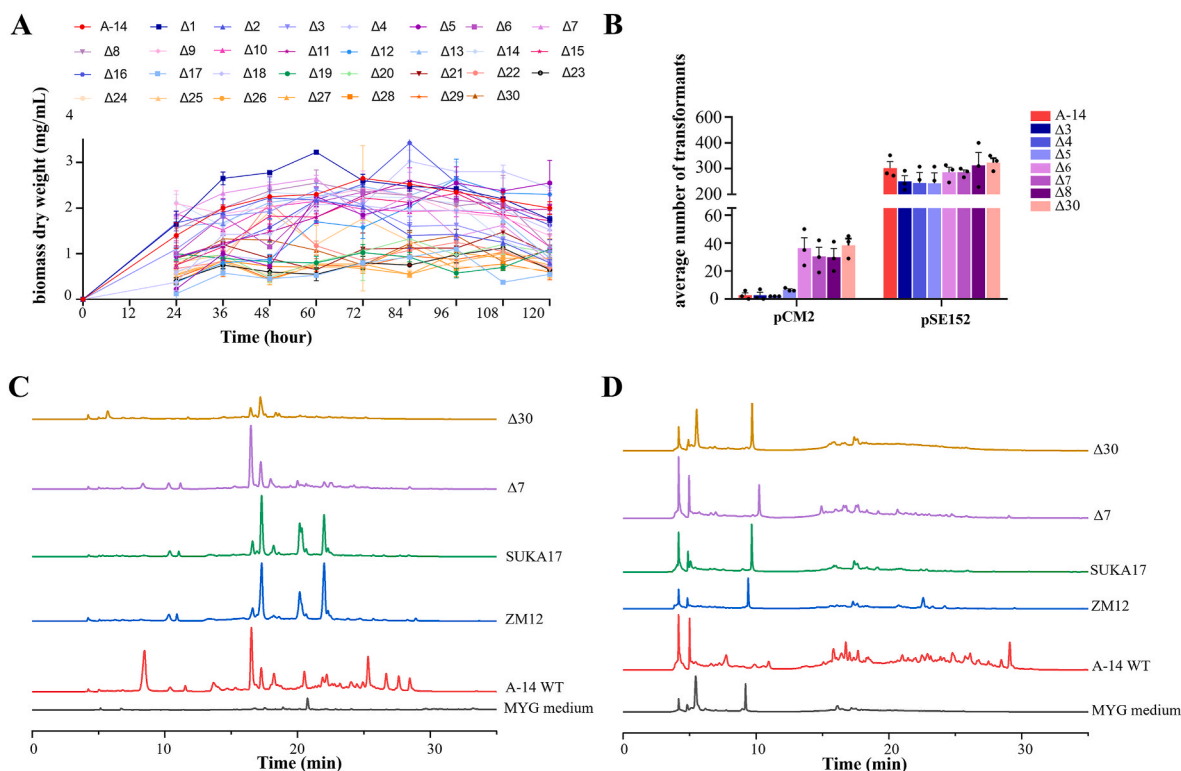
Fig. 4. Characterization of the *Streptomyces* sp. A-14 series genome-reduced mutants. (A) The growth curves of the A-14 WT and the genome-reduced mutants (Δ1-Δ30) were measured by biomass in MYG liquid culture, these results showed that Δ1-Δ17 were similar with WT while Δ18-Δ30 show impaired growth features. (B) The transformation efficiency of pCM2 and pSET152 plasmids in *Streptomyces* sp. A-14 and the mutant stains. (C) HPLC analysis of ethyl acetate extracts of *Streptomyces* sp. A-14 and the engineered strains cultivated in MYG liquid medium. (D) HPLC analysis of 1-butanol extracts of *Streptomyces* sp. A-14 and the engineered strains cultivated in MYG liquid medium.
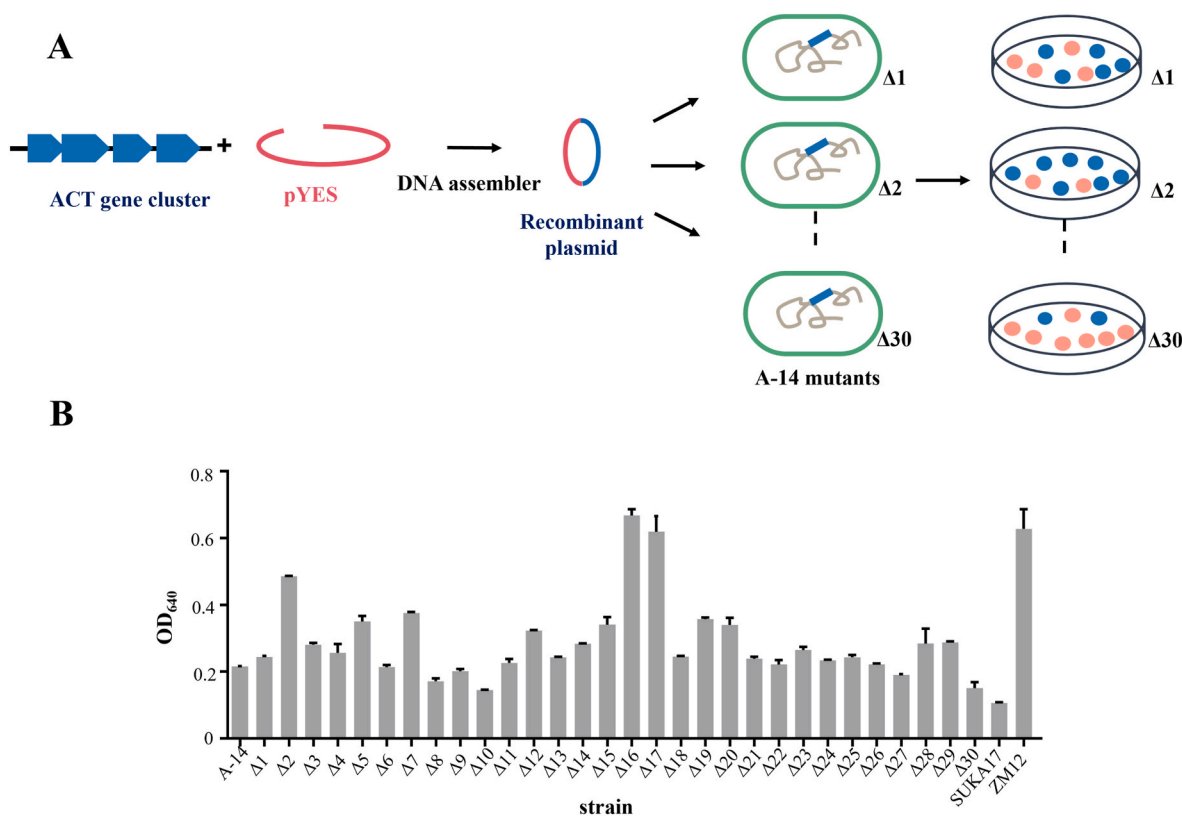
Fig. 5. Cloning of ACT gene cluster in *Streptomyces* chassis (Δ1-Δ30, *S. avermitilis* SUKA17, *S. coelicolor* ZM12) and their application for actinomycin yield analysis. (A) The act gene cluster was reconstructed using yeast homologous recombination-based DNA assembly and the plasmid pYES-ACT was conjured and transferred to the chassis of *Streptomyces*. (B) Analysis of the relative actinomycin yield in different *Streptomyces* chassis using flow cytometry-based quantitative method.

laboratory cultivation conditions. To activate the gene cluster, we inserted a promoter *kasO**p in the upstream of the first biosynthetic gene (gene 1) of the PTM operon to drive the expression of the whole BGC (Fig. S4A). The same promoter was inserted in front of gene 1 in mutant strains (Δ2, Δ5, Δ7, Δ16, Δ17, Δ19, Δ20) harboring the PTM gene cluster. This gene cluster (pYES-PTM) was also reconstructed and transformed into *S. avermitilis* SUKA17 and *S. coelicolor* ZM12 for heterologous expression. (Fig. S4B, Table S5). The RT-PCR results confirmed that all the genes were transcribed under the *kasO**p promoter (Fig. S4C).

The activation of this BGC was confirmed by HPLC analysis with the observation of several new metabolite peaks (Fig. 6B). There were three major compounds compared with the negative control (*Streptomyces* sp. A-14 with the silent PTM gene cluster) [34]. The first PTM peak **a** was observed at around 26–28 min with a corresponding mass of $[M+H]^+ =$ 511.2663, a second PTM peak **b** $[M+H]^+ = 511.2680$, and a third PTM peak **c** $[M+H]^+ = 495.2736$ (Fig. S5). The yield of PTM was indicated by the peak area of compound **a**. The yields of PTM compounds in mutant strains (Δ2, Δ5, Δ7, Δ16, Δ17) were higher than that of *Streptomyces* sp. A-14, *S. coelicolor* ZM12 and *S. avermitilis* SUKA17. The strain Δ16 had a 4.3-fold higher yield than those of *Streptomyces* sp. A-14 (Fig. 6C). Overall, the production of PTM improved in the genome-reduced mutants (Δ2, Δ5, Δ7, Δ16, Δ17), which have similar growth curve with *Streptomyces* sp. A-14 WT and less metabolic background. This suggests that these strains could serve as superior chassis for subsequent genome mining of cryptic BGCs from other actinobacteria.

4. Discussion

Heterologous expression of NP BGCs in genome-reduced mutants of *Streptomyces* has proven to be an efficient method for synthesizing desired compounds, serving as production platforms in industrial applications [35]. The characteristics of several classic model *Streptomyces* chassis suitable for NP discovery and overproduction were compared and summarized in Table S6. In this study, we isolated a fast-growing *Streptomyces* sp. A-14 and engineered it into a genome-reduced host for heterologous expression of NP BGCs. A series of genome-reduced strains were generated by CRISPR/Cas-based engineering techniques to delete most indigenous secondary metabolite BGCs and several nonessential genomic regions located in sub-telomeric regions.

The mutant strains (Δ1-Δ18) show similar growth trends with *Streptomyces* sp. A-14 WT. However, the mutant strains (Δ19-Δ30) exhibited decreased cell growth and biomass, suggesting that the sequential deletion of these gene clusters had a cumulative effect on cell growth. Similar results have been observed in other organisms as well. In *Schlegelella brevitalea* DSM 7029, deletion of the gene clusters severely affected growth, implying that these gene clusters may have certain endogenous functions in cell growth [21]. In the case of *S. chattanoogensis* L320, a 1.3 Mb deletion in the right sub-telomeric region decreased growth rate and caused abnormal mycelial growth, which hindered its suitability as a production platform in industrial applications [36]. Thus, the appropriate elimination of nonessential genomic regions and native BGCs to maintain biotechnological performance could be a feasible strategy to construct a versatile chassis.

In addition, the *Streptomyces* sp. A-14 WT strain grows a yellowish-green aerial mycelium, whereas the aerial mycelium of the chassis strain Δ23-Δ30 were white. The loss of color was observed after deletion of region 14 and 22, respectively. Genome analysis revealed that region 14 contains an isorenieratene gene cluster and region 22 is involved in the biosynthesis of lasalocid, which has an orange color [37]. In *S. albus* J1074, the aerial mycelium color of the engineered strains changed with the deletion of isorenieratene gene cluster as well [17]. These results confirmed that deletion of non-essential BGCs would generate cleaner
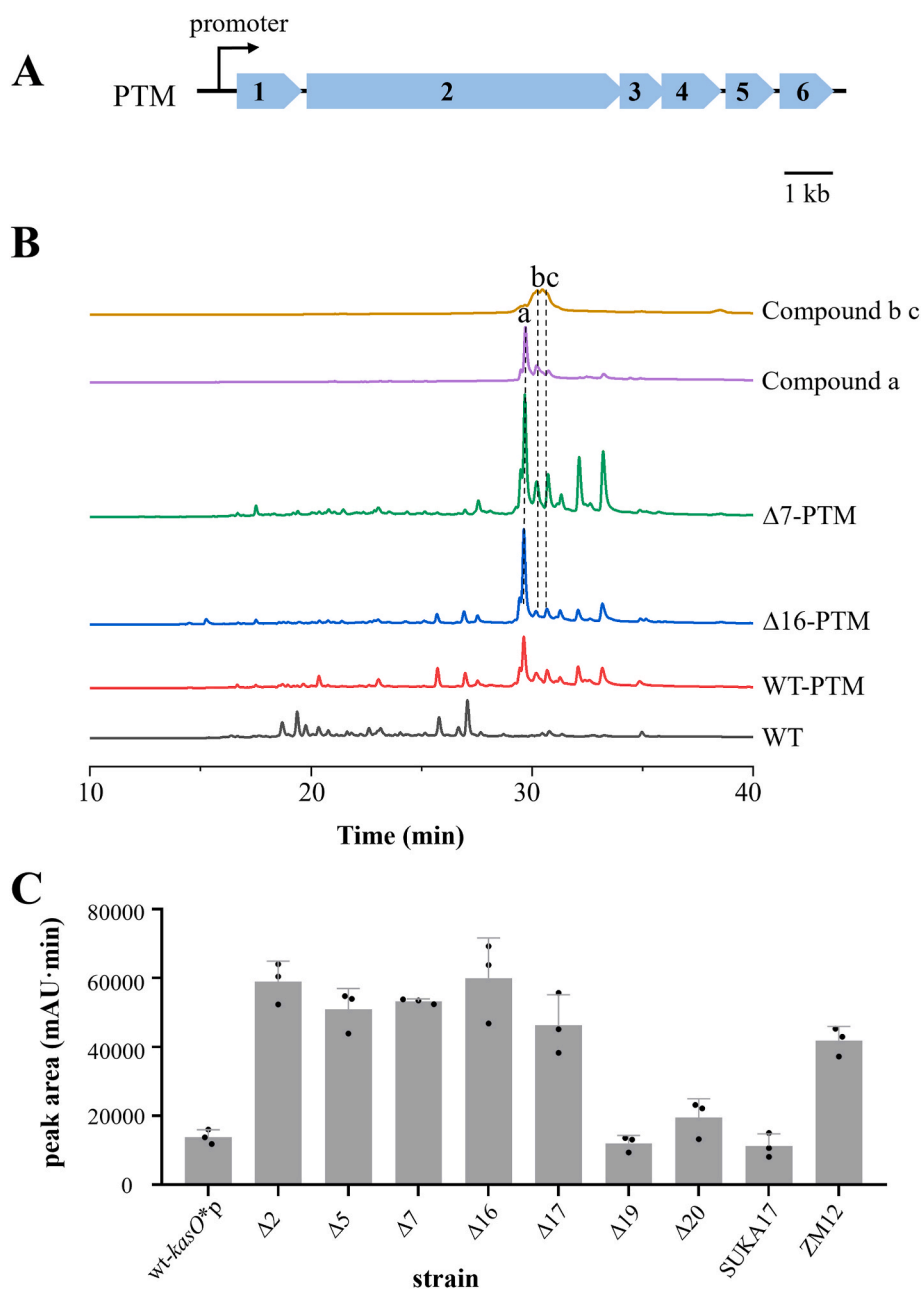
Fig. 6. Activation and heterologous expression of PTMs BGC in genome-reduced chassis. (A) The bioinformatics analysis of PTMs BGC from *Streptomyces* sp. A-14. (B) HPLC analysis of the production of PTM in different chassis. (C) Yield comparison of PTM in A-14 chassis (Δ2, Δ5, Δ7, Δ17, Δ19, Δ20), *Streptomyces* sp. A-14, *S. avermitilis* SUKA17 and *S. coelicolor* ZM12. Data are presented as mean values ± SD. n = 3 biologically independent samples.

metabolic background for future NP purification.

The genome-reduced *Streptomyces* sp. A-14 chassis indeed increased the production of secondary metabolic BGCs. The yields of ACT and PTM in genome reduced strains (Δ2, Δ5, Δ7, Δ16) were higher than those of the *Streptomyces* sp. A-14 WT strain and *S. avermitilis* SUKA17. However, the yields of BGCs in genome reduced strains varied, which may be caused by cumulative deletions affecting the biomass or regulatory of metabolic networks. The engineered *Streptomyces* sp. A-14 chassis (Δ2, Δ5, Δ7, Δ16) displayed fast-growing growth curve, simplified metabolic background, and enhanced expression of BGCs, which suggests that appropriate deletions of BGCs and dispensable genes in *Streptomyces* could be an effective strategy for constructing robust cell factories, facilitating yield improvements and large-scale discovery of novel NPs with unique bioactivities.

Declarations of competing interests

The authors declare no competing interests.

CRediT authorship contribution statement

Hui Li: performed the experiments, wrote the manuscript. **Sheng Gao:** performed the experiments, wrote the manuscript. **Sanyuan Shi:** performed the experiments, wrote the manuscript. **Xiaomin Zhao:** performed the experiments. **Haoyu Ye:** performed the experiments. **Yunzi Luo:** designed and conceptualized the project, wrote the manuscript, All the authors read and approved the final manuscript.

Declaration of competing interest

The authors declare that they have no known competing financial interests or personal relationships that could have appeared to influence the work reported in this paper.

Acknowledgments

We are grateful to Professor Huimin Zhao from the University of Illinois at Urbana-Champaign for providing the plasmid pCRISPomyces-2.

Appendix A. Supplementary data

Supplementary data to this article can be found online at https://doi.org/10.1016/j.synbio.2024.04.017.

References

[1] Harvey AL, Edrada-Ebel R, Quinn RJ. The re-emergence of natural products for drug discovery in the genomics era. Nat Rev Drug Discov 2015;14:111–29. https://doi.org/10.1038/nrd4510.
[2] Wang W, Li S, Li Z, Zhang J, Fan K, Tan G, et al. Harnessing the intracellular triacylglycerols for titer improvement of polyketides in *Streptomyces*. Nat Biotechnol 2020;38:76–83. https://doi.org/10.1038/s41587-019-0335-4.
[3] Li S, Yang B, Tan GY, Ouyang LM, Qiu S, Wang W, et al. Polyketide pesticides from actinomycetes. Curr Opin Biotechnol 2021;69:299–307. https://doi.org/10.1016/j.copbio.2021.05.006.
[4] Rutledge PJ, Challis GL. Discovery of microbial natural products by activation of silent biosynthetic gene clusters. Nat Rev Microbiol 2015;13:509–23. https://doi.org/10.1038/nrmicro3496.
[5] Huang C, Wang C, Luo Y. Research progress of pathway and genome evolution in microbes. Synth Syst Biotechnoly 2022;7:648–56. https://doi.org/10.1016/j.synbio.2022.01.004.
[6] Luo Y, Li BZ, Liu D, Zhang L, Chen Y, Jia B, et al. Engineered biosynthesis of natural products in heterologous hosts. Chem Soc Rev 2015;44:5265–90. https://doi.org/10.1039/c5cs00025d.
[7] Shi S, Xie Y, Wang G, Luo Y. Metabolite-based biosensors for natural product discovery and overproduction. Curr Opin Biotechnol 2022;75:10–26. https://doi.org/10.1016/j.copbio.2022.102699.
[8] Enghiad B, Huang C, Guo F, Jiang G, Wang B, Tabatabaei SK, et al. Cas12a-assisted precise targeted cloning using *in vivo* Cre-lox recombination. Nat Commun 2021;12:1171. https://doi.org/10.1038/s41467-021-21275-4.
[9] Hu YL, Zhang Q, Liu SH, Sun JL, Yin FZ, Wang ZR, et al. Building *Streptomyces albus* as a chassis for synthesis of bacterial terpenoids. Chem Sci 2023;14:3661–7. https://doi.org/10.1039/d2sc06033g.
[10] Yang Z, Liu C, Wang Y, Chen Y, Li Q, Zhang Y, et al. Mgcep 1.0: a genetic-engineered marine-derived chassis cell for a scaled heterologous expression platform of microbial bioactive metabolites. ACS Synth Biol 2022;11:3772–84. https://doi.org/10.1021/acssynbio.2c00362.
[11] Li S, Li Z, Pang S, Xiang W, Wang W. Coordinating precursor supply for pharmaceutical polyketide production in *Streptomyces*. Curr Opin Biotechnol 2021;69:26–34. https://doi.org/10.1016/j.copbio.2020.11.006.
[12] Ke J, Yoshikuni Y. Multi-chassis engineering for heterologous production of microbial natural products. Curr Opin Biotechnol 2019;62:88–97. https://doi.org/10.1016/j.copbio.2019.09.005.
[13] Novakova R, Nunez LE, Homerova D, Knirschova R, Feckova L, Rezuchova B, et al. Increased heterologous production of the antitumoral polyketide mithramycin A by engineered *Streptomyces lividans* TK24 strains. Appl Microbiol Biotechnol 2018;102:857–69. https://doi.org/10.1007/s00253-017-8642-5.
[14] Zhou M, Jing X, Xie P, Chen W, Wang T, Xia H, et al. Sequential deletion of all the polyketide synthase and nonribosomal peptide synthetase biosynthetic gene clusters and a 900-kb subtelomeric sequence of the linear chromosome of *Streptomyces coelicolor*. FEMS Microbiol Lett 2012;333:169–79. https://doi.org/10.1111/j.1574-6968.2012.02609.x.
[15] Komatsu M, Uchiyama T, Omura S, Cane DE, Ikeda H. Genome-minimized *Streptomyces* host for the heterologous expression of secondary metabolism. Proc Natl Acad Sci USA 2010;107:2646–51. https://doi.org/10.1073/pnas.0914833107.
[16] Kallifidas D, Jiang G, Ding Y, Luesch H. Rational engineering of *Streptomyces albus* J1074 for the overexpression of secondary metabolite gene clusters. Microb Cell Fact 2018;17:1–25. https://doi.org/10.1186/s12934-018-0874-2.
[17] Myronovskyi M, Rosenkranzer B, Nadmid S, Pujic P, Normand P, Luzhetskyy A. Generation of a cluster-free *Streptomyces albus* chassis strains for improved heterologous expression of secondary metabolite clusters. Metab Eng 2018;49:316–24. https://doi.org/10.1016/j.ymben.2018.09.004.
[18] Wang B, Guo F, Dong SH, Zhao H. Activation of silent biosynthetic gene clusters using transcription factor decoys. Nat Chem Biol 2019;15:111–4. https://doi.org/10.1038/s41589-018-0187-0.
[19] Blin K, Shaw S, Augustijn HE, Reitz ZL, Biermann F, Alanjary M, et al. antiSMASH 7.0: new and improved predictions for detection, regulation, chemical structures and visualisation. Nucleic Acids Res 2023 Jul;51(W1):W46–50. https://doi.org/10.1093/nar/gkad344.
[20] Choe D, Cho S, Kim SC, Cho BK. Minimal genome: Worthwhile or worthless efforts toward being smaller? Biotechnol J 2016;11:199–211. https://doi.org/10.1002/biot.201400838.
[21] Liu J, Zhou H, Yang Z, Wang X, Chen H, Zhong L, et al. Rational construction of genome-reduced *Burkholderiales* chassis facilitates efficient heterologous production of natural products from proteobacteria. Nat Commun 2021;12:43–7. https://doi.org/10.1038/s41467-021-24645-0.
[22] Kieser T, Bibb MJ, Chater KF, Butter MJ, Hopwood DA, Bittner M. Practical *Streptomyces* genetics: a laboratory manual. 2000. p. 581–5.
[23] Rhoads A, Au KF. PacBio sequencing and its applications. Dev Reprod Biol 2015;13:278–89. https://doi.org/10.1016/j.gpb.2015.08.002.
[24] Koren S, Harhay GP, Smith TP, Bono JL, Harhay DM, McVey SD, et al. Reducing assembly complexity of microbial genomes with single-molecule sequencing. Genome Biol 2013;14:1–16. https://doi.org/10.1186/gb-2013-14-9-r101.
[25] Chin CS, Alexander DH, Marks P, Klammer AA, Drake J, Heiner C, et al. Nonhybrid, finished microbial genome assemblies from long-read SMRT sequencing data. Nat Methods 2013;10:563–9. https://doi.org/10.1038/nmeth.2474.
[26] Kelley DR, Liu B, Delcher AL, Pop M, Salzberg SL. Gene prediction with Glimmer for metagenomic sequences augmented by classification and clustering. Nucleic Acids Res 2012;40:1–9. https://doi.org/10.1093/nar/gkr1067.
[27] Tatusov RL, Galperin MY, Natale DA, Koonin EV. The COG database: a tool for genome-scale analysis of protein functions and evolution. Nucleic Acids Res 2000;28:33–6. https://doi.org/10.1093/nar/28.1.33.
[28] Cobb RE, Wang Y, Zhao H. High-efficiency multiplex genome editing of *Streptomyces* species using an engineered CRISPR/Cas system. ACS Synth Biol 2015;4:723–8. https://doi.org/10.1021/sb500351f.
[29] Shao Z, Zhao H, Zhao H. DNA assembler, an *in vivo* genetic method for rapid construction of biochemical pathways. Nucleic Acids Res 2009;37:1–16. https://doi.org/10.1093/nar/gkn991.
[30] Shima J, Hesketh A, Okamoto S, Kawamoto S, Ochi K. Induction of actinorhodin production by rpsL (encoding ribosomal protein S12) mutations that confer *streptomycin* resistance in *Streptomyces lividans* and *Streptomyces coelicolor* A3(2). J Bacteriol 1996;178:7276–84. https://doi.org/10.1128/jb.178.24.7276-7284.1996.
[31] Hwang S, Lee Y, Kim JH, Kim G, Kim H, Kim W, et al. *Streptomyces* as microbial chassis for heterologous protein expression. Front Bioeng Biotechnol 2021;9:1–23. https://doi.org/10.3389/fbioe.2021.804295.
[32] Kim JN, Kim Y, Jeong Y, Roe JH, Kim BG, Cho BK. Comparative genomics reveals the core and accessory genomes of *Streptomyces* species. J Microbiol Biotechnol 2015;25:1599–605. https://doi.org/10.4014/jmb.1504.04008.
[33] Peng Q, Gao G, Lu J, Long Q, Chen X, Zhang F, et al. Engineered *Streptomyces lividans* strains for optimal identification and expression of cryptic biosynthetic gene clusters. Front Microbiol 2018;9:1–15. https://doi.org/10.3389/fmicb.2018.03042.
[34] Luo Y, Huang H, Liang J, Wang M, Lu L, Shao Z, et al. Activation and characterization of a cryptic polycyclic tetramate macrolactam biosynthetic gene cluster. Nat Commun 2013;4:1–13. https://doi.org/10.1038/ncomms3894.
[35] Hopwood DA. Soil to genomics: the *Streptomyces* chromosome. Annu Rev Genet 2006;40:1–23. https://doi.org/10.1146/annurev.genet.40.110405.090639.
[36] Bu QT, Yu P, Wang J, Li ZY, Chen XA, Mao XM, et al. Rational construction of genome-reduced and high-efficient industrial *Streptomyces* chassis based on multiple comparative genomic approaches. Microb Cell Fact 2019;18:1–16. https://doi.org/10.1186/s12934-019-1055-7.
[37] Myronovskyi M, Tokovenko B, Brotz E, Ruckert C, Kalinowski J, Luzhetskyy A. Genome rearrangements of *Streptomyces albus* J1074 lead to the carotenoid gene cluster activation. Appl Microbiol Biotechnol 2014;98:795–806. https://doi.org/10.1007/s00253-013-5440-6.